Journal of Cerebral Blood Flow & Metabolism (2007) 27, 1235–1247

www.jcbfm.com

Arterial versus total blood volume changes during neural activity-induced cerebral blood flow change: implication for BOLD fMRI

Tae Kim[1], Kristy S Hendrich[1], Kazuto Masamoto[1] and Seong-Gi Kim[1,2]

[1]*Department of Radiology, University of Pittsburgh, Pittsburgh, Pennsylvania, USA;* [2]*Department of Neurobiology, University of Pittsburgh, Pittsburgh, Pennsylvania, USA*

Quantifying both *arterial* cerebral blood volume (CBV_a) changes and *total* cerebral blood volume (CBV_t) changes during neural activation can provide critical information about vascular control mechanisms, and help to identify the origins of neurovascular responses in conventional blood oxygenation level dependent (BOLD) magnetic resonance imaging (MRI). Cerebral blood flow (*CBF*), CBV_a, and CBV_t were quantified by MRI at 9.4 T in isoflurane-anesthetized rats during 15-s duration forepaw stimulation. Cerebral blood flow and CBV_a were simultaneously determined by modulation of tissue and vessel signals using arterial spin labeling, while CBV_t was measured with a susceptibility-based contrast agent. Baseline versus stimulation values in a region centered over the somatosensory cortex were: $CBF = 150 \pm 18$ versus 182 ± 20 mL/100 g/min, $CBV_a = 0.83 \pm 0.21$ versus 1.17 ± 0.30 mL/100 g, $CBV_t = 3.10 \pm 0.55$ versus 3.41 ± 0.61 mL/100 g, and $CBV_a/CBV_t = 0.27 \pm 0.05$ versus 0.34 ± 0.06 ($n = 7$, mean ± s.d.). Neural activity-induced absolute changes in CBV_a and CBV_t are statistically equivalent and independent of the spatial extent of regional analysis. Under our conditions, increased CBV_t during neural activation originates mainly from arterial rather than venous blood volume changes, and therefore a critical implication is that venous blood volume changes may be negligible in BOLD fMRI.
Journal of Cerebral Blood Flow & Metabolism (2007) **27,** 1235–1247; doi:10.1038/sj.jcbfm.9600429; published online 20 December 2006

Keywords: arterial blood volume; CBF regulation; cerebral blood volume; fMRI; somatosensory stimulation; venous blood volume

Introduction

Cerebral blood flow and volume (CBF and CBV) are important indicators of brain physiology, viability, and function. Regional CBF and total CBV (CBV_t) changes have been determined by magnetic resonance imaging (MRI) and positron emission tomography (PET) during global and neural stimulation, and their inter-relationship has been determined in rat, monkey and human brain (Grubb *et al*, 1974; Ito *et al*, 2001*b*; Jones *et al*, 2002; Lee *et al*, 2001; Mandeville *et al*, 1999). Relative CBV_t ($rCBV_t$) and relative CBF ($rCBF$) represent values normalized to baseline, and the relationship between these values is generally described following Grubb's equation (Grubb *et al*, 1974), as $rCBV_t = rCBF^{\kappa}$, where κ is a constant equal to 0.38. However, it is not clear what portion of arterial and venous cerebral blood volume (CBV_a and CBV_v, respectively) changes contribute to CBV_t changes. Since CBV_v comprises ~60% to 80% of CBV_t (Lee *et al*, 2001), biomechanical models of vascular response (such as the balloon model) assume that CBV_v changes dominate during stimulation, while CBV_a changes are minimal (Buxton *et al*, 1998; Mandeville *et al*, 1999); thus, changes in CBV_v have often been assumed to be similar to changes in CBV_t. According to vascular physiology studies, however, local and upstream arterial vessels rigorously dilate during increased neural activity (Iadecola *et al*, 1997). Thus, it would be valuable to know the portion of CBV_a change that contributes to overall stimulus-induced CBV_t change to gain insight into vascular control mechanisms. Additionally, in functional MRI (fMRI), the blood

Correspondence: Dr Seong-Gi Kim, Department of Radiology, University of Pittsburgh Medical School, 3025 East Carson Street, Pittsburgh, Pennsylvania 15203, USA.
E-mail: kimsg@pitt.edu
This study was supported by NIH R01 Grants (EB003375, NS44589) and Biomedical Technological Regional Resource Grant (EB001977) to Pittsburgh NMR Center for Biomedical Research, and was presented in part at the 14th Annual Meeting of the International Society for Magnetic Resonance in Medicine. The 9.4T system was funded in part by an NIH Grant (RR17239).
Received 9 June 2006; revised 2 October 2006; accepted 26 October 2006; published online 20 December 2006

oxygenation level dependent (BOLD) signal is closely dependent on many parameters, including *CBF* and *venous* (not *total*) cerebral blood volume (Ogawa *et al*, 1993). An increase in venous oxygenation level induced by an increase in *CBF* produces an increase in BOLD signals, while an increase in venous blood volume decreases the BOLD effect. Therefore, the separation of CBV_t change into CBV_a and CBV_v changes is helpful for the interpretation of BOLD signals.

To measure the relationship between $rCBV_t$ and relative arterial and venous components ($rCBV_a$ and $rCBV_v$, respectively) at different $PaCO_2$ baseline conditions in rat, Lee *et al* (2001) utilized *in vivo* ^{19}F nuclear magnetic resonance (NMR) spectroscopy after infusion of an oxygen-carrying perfluorocarbon, and found that the change in CBV_a was larger than the CBV_v change. Similarly, CBV_t changes induced by hypercapnia and hypocapnia in human PET measurements have been determined to be mainly caused by changes in CBV_a (Ito *et al*, 2005). However, these previously-determined global stimulation findings may not be applicable to a brain region specifically responding to neural stimulation, because of potential differences in global versus local and chemical versus neural vascular regulation mechanisms.

We therefore investigated the relationship between CBV_a and CBV_t in the rat somatosensory stimulation model. Although most fMRI studies have been performed with α-chloralose anesthesia, we instead chose to use isoflurane because it provides stability of anesthetic depth coupled with simple noninvasive induction (Lukasik and Gillies, 2003); these benefits enabled us to maintain consistent animal physiology during the long duration of these experiments. Baseline *CBF* with isoflurane anesthesia is known to be higher than with α-chloralose (Masamoto *et al*, in press), and has been shown to be similar to that of unanesthesized, awake rats (Maekawa *et al*, 1986). Thus, baseline *CBF* values in our isoflurane studies are expected to higher than for α-chloralose studies. Changes in *CBF*, CBV_a, and CBV_t were quantified at baseline and during stimulation in these fMRI studies. *CBF* and CBV_a were simultaneously determined by a recently-developed MRI technique (Kim and Kim, 2005), which relies on independent MOdulations of TIssue and VEssel (MOTIVE) signals; signal intensity from the blood pool can be changed by arterial spin labeling (ASL), while signal originating from tissue can be selectively varied by magnetization transfer (MT) effects with no detectable change to arterial blood signals. The CBV_a value measured by MOTIVE at 9.4 T represents the blood volume within arterial vessels of all sizes, and includes the portion of capillaries carrying blood water before it exchanges with tissue water; the diameter of arterial vessels in the rat parenchyma ranges from 30 to 40 μm in intracortical arterioles to 4 to 6 μm in capillaries (Nakai *et al*, 1981; Sanders and Orrison, 1995). CBV_t was determined by intravascular infusion of a susceptibility-based contrast agent (Tropres *et al*, 2001; Yablonskiy and Haacke, 1994).

Materials and methods

Animal Preparation and Stimulation

All animal protocols were approved by the University of Pittsburgh Animal Care and Use Committee. Thirteen male Sprague–Dawley rats weighing 350 to 450 g (Charles River Laboratories, Wilmington, MA, USA) were studied; *CBF*, CBV_a, and CBV_t values were measured in seven animals, while only *CBF* and CBV_a values were determined in an additional six animals. The animals were initially anesthetized with ~3% isoflurane in a mixture of O_2 and N_2O gases (1:2). The animals were intubated and the femoral artery and the femoral vein were catheterized. Isoflurane levels were then reduced to 1.3% to 1.5%, and the O_2 and N_2O gases were replaced with air supplemented with O_2 to attain a total O_2 level of ~30% throughout the experiments. The head of the animal was carefully secured in a home-built restrainer before placement in the magnet. Arterial blood pressure and respiration rate were continuously recorded. Blood gases were measured (Stat profile pHOx, Nova Biomedical, MA, USA) and ventilation rate and volume were adjusted accordingly. Rectal temperature was maintained at 37 to 37.5°C.

Electrical stimulation was applied to either the right or the left forepaw using two needle electrodes inserted under the skin between digits 2 and 4 and connected to a constant current stimulation isolator (A365D, World Precision Instruments, Inc., Sarasota, FL, USA), which was triggered by a pulse generator (Master 8, AMPI, Israel). Stimulation parameters for activation studies under isoflurane anesthesia were previously optimized by measurements of field potential, blood flow, and BOLD fMRI (Masamoto *et al*, in press); optimal values were implemented in this study where current = 1.5 to 1.8 mA, pulse duration = 3 msecs, and repetition rate = 6 Hz. The stimulation duration was 15 secs and the inter-stimulation period was > 1 min.

Magnetic Resonance Acquisitions

All MRI measurements were performed on a 9.4 T magnet with bore size of 31 cm diameter, interfaced to a Unity INOVA console (Varian, Palo Alto, CA, USA). The gradient coil was an actively shielded 12-cm inner diameter set with a gradient strength of 40 G/cm and a rise time of 130 μs (Magnex, Abingdon, UK). Two actively detunable radio frequency (RF) coils were used: a butterfly-shaped surface coil was positioned in the neck region for ASL, while a surface coil of 2.3 cm diameter was positioned on top of the head, both for tissue saturation via MT effects and for image acquisition. The homogeneity of the magnetic field was manually optimized on a slab twice the thickness of the imaging slice. All coronal images were acquired using single-shot echo planar imaging techniques with slice thickness = 2 mm, matrix

size = 64 (readout) × 32 (phase-encode), and field of view = 3.0 × 1.5 cm^2.

Measurements of cerebral blood flow and arterial cerebral blood volume using the MOTIVE method: A MOTIVE method (ASL with MT) was implemented to measure baseline *CBF* and CBV_a values and their corresponding changes during somatosensory stimulation. In ASL, blood water spins are labeled at the carotid arteries, then this label is carried though arterial vessels and into the capillaries where the exchange between blood and tissue water occurs. If labeled water in capillary blood freely exchanges with tissue water, and spin relaxation is ignored, the contribution of labeled water in capillary blood, tissue, and venous blood will be identical, and so these three compartments are treated together as one compartment. Furthermore, T_2 of venous blood at 9.4 T (5–7 msecs) is very short relative to T_2 of tissue and arterial blood (40 msecs) (Lee *et al*, 1999), and therefore, even if labeled water in capillaries does not completely exchange with tissue water, signal contribution of any remaining labeled water in venous blood will be minimal when TE > 3 times T_2 of venous blood. Since there is minimal label remaining in venous blood, venous blood volume does not contribute to CBV_a values determined by MOTIVE at 9.4 T. Therefore, it is assumed that signal in an imaging voxel originates from only two compartments: arterial blood and tissue.

The experimental design and pulse sequence have been described previously (Kim and Kim, 2005). Arterial-spin labeled and unlabeled images at each of three different MT levels were acquired with an adiabatic-version spin-echo (SE) echo planar imaging sequence (Lee *et al*, 1999). On alternate acquisitions, RF pulses were transmitted from the neck coil at either −8500 Hz in the presence of a 1 G/cm B_0 gradient (for labeled data), or at +8500 Hz with the same B_0 gradient (for unlabeled data). Tissue signals were differentially reduced without changing ASL efficiency by adjusting the RF power level of MT-inducing pulses, which were transmitted from the head coil at +8500 Hz. The MT ratios (MTRs) ($1-(S_{MT}/S_0)$, where S_{MT} and S_0 are equilibrium signals in the presence and absence of MT, respectively) were targeted to values of 0, 0.3, and 0.5 for gray matter, and applied in randomized order (their respective B_1 field strengths were 0, 0.11, and 0.16 G). The spin preparation period was 2.4 s, which includes interleaved ASL and MT pulses, and the repetition time (TR) was 2.5 s. Although the MR signal may not reach steady state during a single spin preparation period, virtually continuous repetition of spin preparation during fMRI studies ensured steady-state MT conditions (acquisition time ≪ spin-preparation time). TE was 40 msecs in the seven studies where CBV_t was subsequently measured, and 30 msecs in the other six studies.

Sixteen pairs of arterial-spin labeled (*lab*) and unlabeled (*unlab*) images were acquired for each MTR; five pairs during prestimulus baseline, three pairs during stimulation and eight pairs during the poststimulus period. The acquisition order of *lab* and *unlab* images was changed in alternate runs; the image order in run *A* was $unlab_{A1}$, lab_{A1}, $unlab_{A2}$, …, lab_{A16}, while in run *B* it was lab_{B1}, $unlab_{B1}$, lab_{B2}, …, $unlab_{B16}$, where subscripts refer to both the run and the pair. Thus, one cycle consisted of six combinations (two acquisition runs × three MTRs). Each full cycle was repeated 20 to 30 times.

Measurement of total cerebral blood volume using a contrast agent: The susceptibility contrast of dextran-coated super paramagnetic iron oxide particles (SPIO) was utilized for the determination of CBV_t at baseline and during somatosensory stimulation. Super paramagnetic iron oxide (whole particle diameter ~30 nm (Dodd *et al*, 1999), obtained from Chien Ho's laboratory at Carnegie Mellon University) was prepared for intravenous injection at a concentration of 15 mg Fe/kg body weight. CBV_t-weighted fMRI studies were performed by acquisition of gradient-echo (GE) echo planar images with TR = 1 s, and TE = 20 and 10 msecs before and after MION injection, respectively. For each condition (without and with SPIO), 70 images were acquired: 10 during prestimulus baseline, 15 during stimulation, and 45 during the poststimulus period. Stimulation runs were repeated 10 to 15 times. Additionally, separate GE echo planar images were acquired without stimulation before and after SPIO injection with TE = 20 msecs for determination of the change in apparent transverse relaxation rate induced by SPIO ($\Delta R^*_{2,agent}$).

At the end of CBV_t-weighted fMRI measurements, blood was withdrawn from the femoral artery to determine the magnetic susceptibility effect of SPIO in blood (Tropres *et al*, 2001). An assembly of perpendicularly oriented tubes had been previously constructed; two capillary tubes (1.1 mm inner diameter and 0.2 mm wall thickness; Fisher Scientific, Pittsburgh, PA, USA) filled with normal saline to ~14 mm length were secured inside an empty large cylinder (12.7 mm inner diameter, 15.0 mm height). The withdrawn blood was immediately placed in this assembly and positioned in the magnet such that one of the capillaries was oriented parallel to B_0, while the other was perpendicular to B_0. Localized spectra were acquired to measure the frequency difference between the peaks originating from each of the capillaries. Blood gas and hematocrit (*Hct*) levels were measured before and after spectroscopy measurements.

Data Processing

General Data Processing: For each animal, *all* identical-condition runs were averaged to generate group data. Then, for the purpose of *inter-animal* comparison only, an exclusion criterion was established. This was necessary because there was a drift in animal physiology of unknown origin during the long experimental durations, making it necessary to adjust the ventilation rate and volume between runs to maintain a constant end-tidal CO_2 level, and consequently, some runs had extremely high or low functional responses. To identify these abnormal fMRI runs, stimulus-induced signal changes were initially calculated within a 9-pixel contralateral region of interest (ROI) for each run (see below for selection of ROIs), and a mean and s.d. value was then determined from all identical-condition runs. Then only identical-condition

runs whose stimulus-induced changes were within the range of the aforementioned ROI-based mean $\pm$ 1.5 s.d. were averaged for the *inter-animal* comparisons.

To determine blood flow and volume changes four time periods were considered. The stimulation period was defined as the time between 5 and 15 secs after the onset of stimulation. Since CBV_t is known to have a slow return to baseline after the cessation of stimulation (Mandeville *et al*, 1999), poststimulation data were divided into consecutive time intervals of 20 secs each, representing early and delayed poststimulation periods. For this reason, only the prestimulation time was defined as the baseline period.

Two types of quantitative analyses were then performed; maps were generated from pixel-by-pixel analysis with 2D Gaussian smoothing, and regional analysis was performed without spatial smoothing. Functional maps were obtained using a boxcar cross-correlation (CC) method (Bandettini *et al*, 1993). Statistical analyses were performed using paired *t*-tests (Origin 7.0, Northampton, MA, USA). All data are reported as mean $\pm$ s.d.

Calculation of cerebral blood flow and arterial cerebral blood volume: Data acquired in runs *A* and *B* were combined at each MT level to obtain unlabeled (S_{MT}) and difference ($\Delta S_{MT} = unlab - lab$) images for matched time spans. It should be noted that S_{sat} and ΔS_{sat} in our original MOTIVE paper (Kim and Kim, 2005) are replaced with S_{MT} and ΔS_{MT} here. S_{MT} images were obtained as $(unlab_{A1} + unlab_{B1})/2$, $(unlab_{A2} + unlab_{B1})/2$, $(unlab_{A2} + unlab_{B2})/2$, etc. Similarly, ΔS_{MT} images were obtained by subtraction of labeled from unlabeled data as $[(unlab_{A1} + unlab_{B1}) - (lab_{A1} + lab_{B1})]/2$, $[(unlab_{A2} + unlab_{B1}) - (lab_{A1} + lab_{B2})]/2$, $[(unlab_{A2} + unlab_{B2}) - (lab_{A2} + lab_{B2})]/2$, etc. In this manner, images were reconstructed for each MT level as follows: the entire prestimulation period yielded nine S_{MT} and nine ΔS_{MT} baseline images; the period from 5 to 15 secs after stimulus onset yielded four S_{MT} and four ΔS_{MT} stimulation images; the initial 20 secs after stimulus offset yielded seven S_{MT} and seven ΔS_{MT} early poststimulus images; and data obtained from the final 20 secs after stimulation offset yielded seven S_{MT} and seven ΔS_{MT} delayed poststimulus images. Then, normalized ΔS_{MT} signals ($\Delta S_{MT}/S_0$) for each of the three MT levels were linearly fitted against normalized unlabeled signals (S_{MT}/S_0) at the corresponding MT level (Kim and Kim, 2005), where S_0 is the signal intensity of an unlabeled image obtained in the absence of MT.

Cerebral blood flow (in units of mL/g/sec) without any arterial blood volume contribution was determined from the fitted data as

$$CBF = \frac{\lambda}{T_1}\left(\frac{slope/\zeta}{2\alpha_c - slope/\zeta}\right) \quad (1)$$

where λ is the tissue-blood partition coefficient of 0.9 mL/g (Herscovitch and Raichle, 1985); T_1 is the T_1 value of tissue without MT and in the absence of *CBF* contributions, which is 2.0 secs (Kim and Kim, 2005); α_c is the labeling efficiency of arterial spins at the capillary exchange site within the imaging slice (as measured with identical experimental parameters), which is 0.31 (Kim and Kim, 2005). The correction term (ζ) in Equation (1) corrects for insufficient relaxation, since labeled and unlabeled images were acquired in an interleaved manner, and since the spin-labeling time was much less than 3 times T_1^* (Barbier *et al*, 2001); $\zeta = (1 - e^{-T_{lab}/T_1^*})$, where T_{lab} is the time span for the spin-preparation period (2.4 secs); and T_1^* is the apparent T_1 value of tissue without MT but including *CBF* contributions, which is $\sim$1.9 secs (Kim and Kim, 2002).

CBV_a (in units of mL/g) can be obtained from the intercept and slope of the aforementioned fitting as

$$CBV_a = \lambda \times intercept/(2\alpha_a - slope) \quad (2)$$

where α_a is the labeling efficiency of spins entering the imaging slice, which is 0.36 (Kim and Kim, 2005).

Calculation of total cerebral blood volume and relative total cerebral blood volume change: Baseline CBV_t was mapped first. Baseline CBV_t quantification requires independent determinations of the effect of SPIO on magnetic susceptibility and the effect of SPIO on the *in vivo* relaxation rate. The effect of SPIO on magnetic susceptibility was measured in the arterial blood withdrawn at the end of studies. All susceptibility values are expressed in CGS units. The spectroscopic frequencies of water peaks originating from our parallel and perpendicularly-oriented capillaries ($v_{||}$ and $v_{\perp}$, respectively) immersed in the withdrawn blood differ because of both hemoglobin in red blood cells and SPIO in plasma, and their separation can be expressed as $v_{||} - v_{\perp} = 2\pi\,\Delta\chi_{blood+agent} \cdot v_0$ (Chu *et al*, 1990; Spees *et al*, 2001), where $\Delta\chi_{blood+agent}$ is the susceptibility difference between the arterial blood containing SPIO and water, and v_0 is the spectrometer resonance frequency, which is 400.37 MHz in this study. Since the susceptibility of plasma is similar to that of water (Weisskoff and Kiihne, 1992), the susceptibility effect of the agent in plasma ($\Delta\chi_{agent}$) can then be determined for each animal from the relationship, $\Delta\chi_{blood+agent} = Hct \cdot [Y\Delta\chi_{oxy} + (1-Y)\Delta\chi_{deoxy}] + (1-Hct)\Delta\chi_{agent}$, where *Hct* was experimentally measured; *Y* is the oxygenation level of blood; $\Delta\chi_{oxy}$ and $\Delta\chi_{deoxy}$ are the susceptibility differences between fully oxygenated red blood cells and water and between fully deoxygenated red blood cells and water, respectively. Since arterial blood is fully oxygenated, the $\Delta\chi_{deoxy}$ term was ignored and the $\Delta\chi_{oxy}$ value was set equal to -0.026 ppm (Weisskoff and Kiihne, 1992). For the condition where static dephasing is dominant, the change in apparent transverse relaxation rate in tissue because of contrast agent in the absence of stimulation ($\Delta R^*_{2,agent}$) can be described (Yablonskiy and Haacke, 1994) as

$$\Delta R^*_{2,agent} = \frac{4}{3}\pi \cdot (1 - Hct) \cdot v_{CBV} \cdot \Delta\chi_{agent} \cdot \gamma B_0 \quad (3)$$

where v_{CBV} is the fractional whole blood volume (mL blood/mL brain), which includes both plasma and blood cells, γ is the gyromagnetic ratio, which is 2.675×10^8 rad/(s T), and $B_0 = 9.4$ T in this study. $\Delta R^*_{2,agent}$ was determined from $\ln(S_{pre}/S_{post})/TE$, where S_{pre} and S_{post} are the signal intensities measured without stimulation at TE = 20 msecs before and after injection of SPIO. Baseline v_{CBV} (mL/mL) was determined from Equation (3) for each

animal from $\Delta R^*_{2,\ \mathrm{agent}}$, and from *Hct* and $\Delta\chi_{\mathrm{agent}}$ obtained from arterial blood. These v_{CBV} values were then converted to baseline CBV_t (mL/g) values by dividing by the density of 1.06 g/mL (Herscovitch and Raichle, 1985).

Absolute CBV_t changes (ΔCBV_t) during stimulation were determined after first calculating the stimulus-induced percentage changes in CBV_t as follows. In fMRI studies, stimulus-induced apparent transverse relaxation rate changes ($\Delta R^*_{2,\mathrm{stim}}$ and $\Delta R^*_{2,\mathrm{stim+agent}}$, without and with SPIO, respectively) were calculated from $-(\Delta S/S)/TE$, where $\Delta S/S$ represents the percentage signal change (stimulation versus baseline). An increase in CBV_t decreases CBV_t-weighted fMRI signals, while a simultaneous oxygenation increase reduces the magnitude of observed CBV_t-weighted changes. The deoxyhemoglobin contribution must therefore be removed for accurate CBV_t quantification based on stimulus-induced response. This was accomplished by calculation as percentage change in $CBV_t = (\Delta R^*_{2,\mathrm{stim+agent}} - \Delta R^*_{2,\mathrm{stim}})/\Delta R^*_{2,\mathrm{agent}}$ (Kennan *et al*, 1998; Zhao *et al*, 2006). Then, absolute CBV_t values during stimulation were calculated by multiplying absolute baseline CBV_t values by stimulus-induced percentage changes in CBV_t.

Selection of regions of interest: The size of the forelimb somatosensory cortical area is $\sim 1.5 \times 1.5\,\mathrm{mm}^2$, based on coronal plates from a rat brain atlas (Paxinos and Watson, 1986) at positions 0.2 and 0.3 mm from bregma. Therefore, 9-pixel square ROIs ($1.4 \times 1.4\,\mathrm{mm}^2$) were defined, where one was centered over the anatomically defined somatosensory cortex on the side contralateral to stimulation (and hereafter referred to as the 'focus' ROI) and the other was positioned on the side ipsilateral to stimulation. Additional ROIs were defined to include a larger area on the side contralateral to stimulation, and thus remove any potential spatial bias: one ROI consisted of pixels where CBV_t maps showed $CC \geq 0.4$, while another ROI was similarly defined, but the previously described 9-pixel inner region was not included. For ROI analyses, all pixels within the ROI were averaged, regardless of whether pixels were active.

Error propagation analysis: Error propagation analysis was performed for the measurement of baseline and stimulation *CBF*, CBV_a, and CBF_t values. For each animal, baseline time points were selected for the calculation of error propagation from the averaged time course (data used for the *inter-animal* comparisons). For *CBF* and CBV_a, the slope and intercept (used in Equations (1) and (2)) obtained from linear fitting of three MT levels for each time point were calculated, and then mean and s.d. of baseline time points were determined. Additional *CBF* and CBV_a errors were propagated based on our errors measured previously (Kim and Kim, 2005, 2006); s.d. is 23.2% of its mean for α_c *and* α_a, and 3% for tissue T_1. For baseline CBV_t, mean and s.d. of baseline time points were determined for conditions without and with SPIO. Another CBV_t error was propagated from *Hct* levels determined before and after spectroscopy measurements and SPIO-induced frequency shifts determined from multiple spectroscopy measurements of the same blood sample. It is assumed that errors during stimulation are the same as for the baseline condition. Then, the error for ΔCBF, ΔCBV_a, and ΔCBF_t was propagated based on errors for baseline and stimulation values.

Results

All animals were maintained within normal physiological ranges; $PaCO_2 = 38.1 \pm 4.6$ mm Hg, $PaO_2 = 110.2 \pm 11.6$ mm Hg, and mean arterial blood pressure = 93.1 ± 8.0 mm Hg ($n = 13$). No significant blood pressure changes were observed during somatosensory stimulation. In the seven animals where SPIO was injected, comparison of *Hct* values before and after spectroscopy measurements on the withdrawn arterial blood show that there was no red blood cell precipitation. The average *Hct* level was $35.9\% \pm 0.9\%$ ($n = 7$). The susceptibility effect of blood and agent ($\Delta\chi_{\mathrm{blood+agent}}$) after SPIO injection was 0.23 ± 0.02 ppm (corresponding to an average frequency shift of ~ 570 Hz) and the susceptibility effect of SPIO in plasma ($\Delta\chi_{\mathrm{agent}}$) was 0.36 ± 0.03 ppm ($n = 7$). The average baseline transverse relaxation rate change induced by SPIO ($\Delta R^*_{2,\mathrm{agent}}$) determined from multiple measurements in each animal in the 'focus' ROI was $80.1 \pm 14.8\,\mathrm{secs}^{-1}$ ($n = 7$). Baseline signal changes were minimal during the 2 to 3 h required for measurements after injection of SPIO. This is consistent with a prior observation that there were no ΔR^*_2 changes over a 3-h period in rat brain (Mandeville *et al*, 1997). Using Equation (3) with $\Delta R^*_{2,\mathrm{agent}}$, $\Delta\chi_{\mathrm{agent}}$, and *Hct*, baseline fractional total blood volume (v_{CBV}) was found to be 3.28 ± 0.59 mL/100 mL ($n = 7$).

Baseline *CBF*, CBV_a, and CBV_t maps were successfully obtained from all measurements, as well as functional maps corresponding to somatosensory stimulation. Results for three animals appear in Figures 1A–1C, where the grayscale maps are baseline values, and color overlays represent functional activation. The ventral brain region was relatively far from the detection coil, resulting in poor sensitivity, and likely large errors in *CBF*, CBV_a, and CBV_t quantification. Baseline maps in all three animals (Figures 1A–1C) were quite similar, except at the cortical surface area where large vessels exist. CBV_a and CBV_t maps show apparent differences in the deep gray matter (including thalamus) regions, which may be caused by structural differences in tissue supplied by striate arteries, use of constant λ, T_1, and α_a values for generating CBV_a maps, or smearing from the susceptibility effect of the contrast agent. Baseline values for *CBF*, CBV_a, and CBV_t are higher in gray matter than in white matter, as expected. During stimulation, localized activation was observed in the contralateral somatosensory cortex. Since the CC value is dependent on sensitivity, the size of the activation area also depends on the threshold chosen for display. Functional activation maps of CBV_t for matched

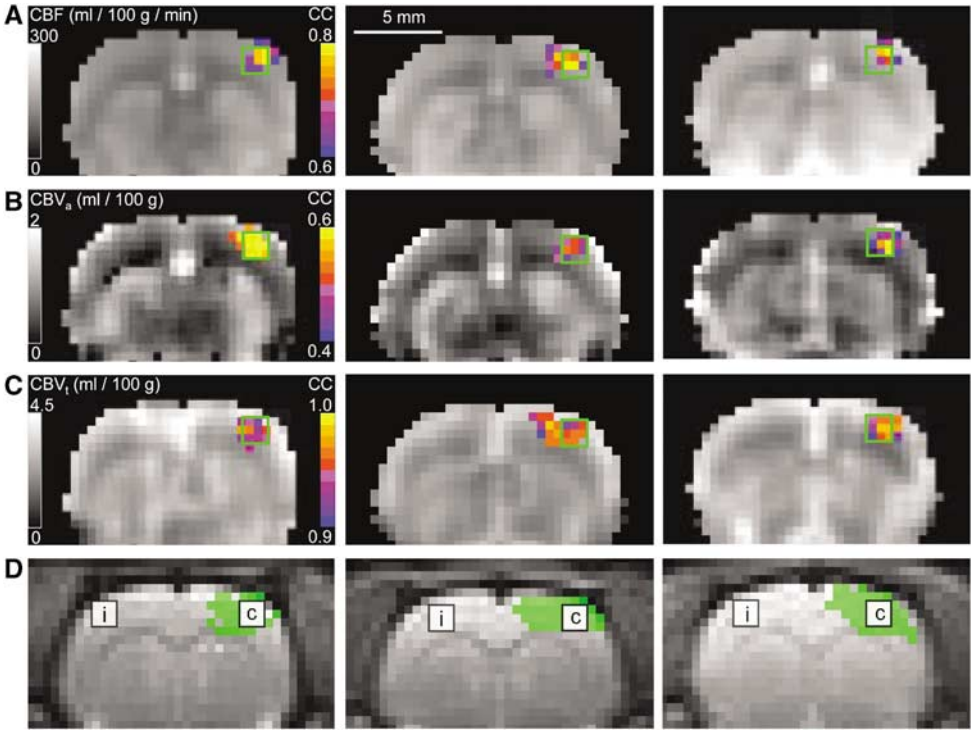

Figure 1 Quantitative baseline hemodynamic maps and the corresponding responses to somatosensory stimulation for three different animals (columns). The hemisphere contralateral to stimulation appears on the right side of all images. Functional activation maps are overlaid in color on the grayscale baseline maps from measurements of *CBF* (**A**), CBV_a (**B**) and CBV_t (**C**). Maps were calculated after application of 2D Gaussian filter (full-width half-maximum = 2 pixels). The gray scale bars (left side) show quantification values for the baseline maps. Baseline values in all maps are higher in gray matter than in white matter. Color scale bars (right side) show correlation coefficients for functional maps, and the green square indicates boundaries of the 9-pixel ROIs centered over the anatomically defined somatosensory cortex in the contralateral hemisphere ('focus' ROIs). Since the CC value is dependent on sensitivity, the size of the activation depends on the threshold chosen for display. The hemodynamic measurement techniques have different sensitivities, so the color bar scale was adjusted in *CBF*, CBV_a, and CBV_t maps to roughly match the size of activation area between techniques. However, the focus of activation is consistent in all three hemodynamic maps. Similar observations were detected in all animals. (**D**) ROIs chosen for regional analysis are overlaid on echo planar images. The 9-pixel ROIs are shown as white boxes and marked with 'c' or 'i', for contralateral and ipsilateral sides, respectively. 'CBV_t-active' ROIs (pixels where CC$\geqslant$0.4 in CBV_t maps) appear as green areas plus white boxes marked 'c', while 'CBV_t-active minus focus' ROIs (area away from activation focus) are just the green areas.

display thresholds would therefore show the largest regions of activation, because the CBV-weighted fMRI technique has higher sensitivity than the MOTIVE method with ASL. However, the focus of activation is consistent for *CBF*, CBV_a, and CBV_t. Similar observations were detected in all animals.

Regional quantification of *CBF*, CBV_a, and CBV_t values was performed without spatial smoothing for baseline and stimulation periods. Location of ROIs chosen for analysis is shown on echo planar images (Figure 1D), where this lack of smoothing clearly resolves gray and white matter boundaries. The 'focus' ROIs centered over the anatomically defined somatosensory cortex on the side contralateral to stimulation appear in Figure 1D as white boxes marked 'c', while 9-pixel ROIs on the side ipsilateral to stimulation appear as white boxes marked 'i'. Average baseline and stimulation values ($n=7$) from 'focus' ROIs are reported in Table 1. The average ratio of CBV_a to CBV_t within the 'focus' ROI was 0.27 $\pm$0.05 for baseline and 0.34$\pm$0.06 for stimulation. Regional baseline values of *CBF*, CBV_a, and CBV_t were also measured in the 9-pixel ROI on the ipsilateral side: $CBF = 146 \pm 20$ mL/100 g/min, $CBV_a = 0.87 \pm 0.32$ mL/100 g and $CBV_t = 3.18 \pm 0.41$ mL/100 g ($n=7$). Baseline values in these contralateral versus ipsilateral ROIs for *CBF*, CBV_a, and CBV_t were not statistically different ($P>0.05$). With inclusion of the six studies in which CBV_t was not measured, *CBF* and CBV_a values within the 'focus' ROI were 151 ± 23 mL/100 g/min and 0.90 ± 0.25 mL/100 g ($n=13$) for baseline, and 196 ± 33 mL/100 g/min and 1.32 ± 0.39 mL/100 g ($n=13$) for stimulation. It should be noted that autoradiography measurements in the rat somatosensory cortex yielded a *CBF* value of 147 mL/100 g/min for 1.38% isoflurane anesthesia (Maekawa *et al*, 1986). Changes in *CBF* and CBV_t (22% and 10%) in our isoflurane-anesthetized studies are less than values observed previously under α-chloralose anesthesia (Mandeville *et al*, 1998; Silva *et al*, 2000), which is likely because of the difference in anesthetics.

Table 1 Measured parameters and changes due to activation within the 'focus' ROI ($n = 7$, mean $\pm$ s.d.)[a]

	CBF (mL/100 g/min)	CBV_a (mL/100 g)	CBV_t (mL/100 g)[b]
Baseline (prestimulation)	150 ± 18 (*148 ± 18*)	0.83 ± 0.21 (*0.86 ± 0.21*)	3.10 ± 0.55 (*3.10 ± 0.55*)
Stimulation	$182 \pm 20^{*}$ (*182 ± 18*)*	$1.17 \pm 0.30^{*}$ (*1.20 ± 0.26*)*	$3.41 \pm 0.61^{*}$ (*3.42 ± 0.59*)*
Early poststimulation	150 ± 20^{NS}	0.86 ± 0.20^{NS}	$3.22 \pm 0.57^{*}$
Delayed poststimulation	144 ± 19^{NS}	0.84 ± 0.13^{NS}	$3.11 \pm 0.56^{+}$
Absolute change[c]	32 ± 8 (*34 ± 12*)	0.34 ± 0.16 (*0.35 ± 0.10*)	0.31 ± 0.11 (*0.32 ± 0.10*)
Percentage change[d]	22 ± 6 (*23 ± 9*)	41 ± 16 (*42 ± 10*)	10 ± 3 (*10 ± 3*)

[a]Results of averaging *all* data for comparison of *CBF*, CBV_a, and CBV_t appear first, while results of averaging only the data within ± 1.5 s.d. for later *inter-animal* comparison follow in parenthesis and italicized. Data obtained during stimulation and poststimulation periods were compared with baseline data (paired *t*-test): NS, not significant; $^{+}P < 0.05$; $^{*}P < 0.01$.

[b]$CBV_{t\,stimulation} = CBV_{t\,baseline}$ (1 + percentage change in CBV_t), where percentage change in CBV_t was determined after removal of the deoxyhemoglobin contribution (see text).

[c]Absolute changes (Δ) were calculated by subtracting baseline (prestimulation) from stimulation signals, for example: $\Delta CBV_a = CBV_{a\,stimulation} - CBV_{a\,baseline}$.

[d]Stimulation-induced percentage changes (%) were calculated by absolute changes/baseline values.

From *CBF* and CBV, mean transit time of blood (MTT) can be calculated as MTT (min) = CBV (mL/100 g)/*CBF* (mL/100 g/min), using the central volume principle. For the 'focus' ROI, the mean arterial transit time (MTT_a) (i.e., the time for blood to travel through arterial volumes within a pixel) was 336 ± 95 msecs for baseline and 388 ± 99 msecs for stimulation, while the mean total transit time of blood (MTT_t) (i.e., the time for blood to travel through the total vasculature within a pixel) was 1271 ± 347 msecs for baseline and 1140 ± 269 msecs for stimulation ($n = 7$). Thus, the stimulus-induced changes in *MTT* (ΔMTT) are $+53 \pm 34$ msecs for arterial vasculature and -131 ± 100 msecs for total vasculature. Since average blood velocity is related to the inverse of MTT, the negative values of ΔMTT_t indicate a stimulus-induced increase in total blood velocity, while the small ΔMTT_a values suggest there is minimal change to arterial blood velocity.

The relationship between CBV_a and CBV_t was also determined in the 'focus' ROI during two consecutive poststimulation recovery periods (Table 1). Values for baseline (pre-stimulation) CBV_a versus both early and delayed poststimulation CBV_a were not statistically different ($P > 0.05$). However, both post-stimulation CBV_t values were significantly higher than baseline CBV_t (Table 1). This suggests that there is a slow return of CBV_t to prestimulation baseline levels after stimulation offset, which is consistent with previous observations in the rat somatosensory cortex (Mandeville *et al*, 1999).

The absolute change in CBV_a (ΔCBV_a) because of activation in the 'focus' ROI was 0.34 ± 0.16 mL/100 g, while the CBV_t change (ΔCBV_t) was 0.31 ± 0.11 mL/100 g (Table 1). The statistical difference between stimulation-induced ΔCBV_a versus ΔCBV_t is not significant (paired *t*-test, $P = 0.38$); however, the active region always appeared larger in CBV_t than in *CBF* and CBV_a functional maps displayed with the same CC threshold, and therefore the size of ROI chosen for analysis could potentially bias our results. To examine the consistency of the quantitative relationship between *CBF*, CBV_a, and CBV_t values were also analyzed within a larger ROI encompassing pixels where CC $\geqslant 0.4$ in CBV_t maps. This region includes 33 ± 6 pixels ($n = 7$) and is referred to as the 'CBV_t-active' ROI (shown in Figure 1D as the area of green pixels plus the white boxes marked 'c'). It should be noted that this includes all pixels of *CBF* and CBV_a activation for the same threshold. Values were also quantified for an area away from the activation focus; this ROI was defined as pixels in the 'CBV_t-active' ROI outside of the 'focus' ROI (the area covered by only the green pixels in Figure 1D). This region includes 24 ± 5 pixels ($n = 7$) and is referred to as the 'CBV_t-active minus focus' ROI. The absolute change in these larger ROIs was smaller compared with the 'focus' ROI because of a partial volume effect (Figure 2A). However, even in these larger regions, ΔCBV_a versus ΔCBV_t is not statistically different (Figure 2A). The ratio of relative values for CBV_t to CBV_a is also consistent; 0.78 ± 0.07 in the 'focus' ROI versus 0.85 ± 0.07 in the 'CBV_t-active ROI' versus 0.87 ± 0.08 in the 'CBV_t-active minus focus' ROI (no statistical difference, $P > 0.05$) (Figure 2B). This demonstrates that the choice of ROI does not change the relationship between CBV_a and CBV_t.

Inter-animal comparisons of *CBF*, CBV_a, and CBV_t baseline and stimulation values were made for runs whose mean stimulus-induced changes were within the range of the mean ± 1.5 s.d.; these values within the 'focus' ROI were averaged across all animals and appear in parenthesis in Table 1. Averaged values with and without this exclusion criterion were not different ($P > 0.05$). *Inter-animal* comparisons of *CBF*, CBV_a and CBV_t baseline and stimulation values within the 'focus' ROI are plotted in Figures 3A and 3B, while stimulus-induced changes in absolute values (ΔCBF, ΔCBV_a, and ΔCBV_t) are plotted in Figures 3C and 3D. Although inter-animal variation still causes scatter in the data (Figures 3A and 3B), *CBF*, CBV_a, and CBV_t values for all animals are increased during stimulation (Figures 3C and 3D),

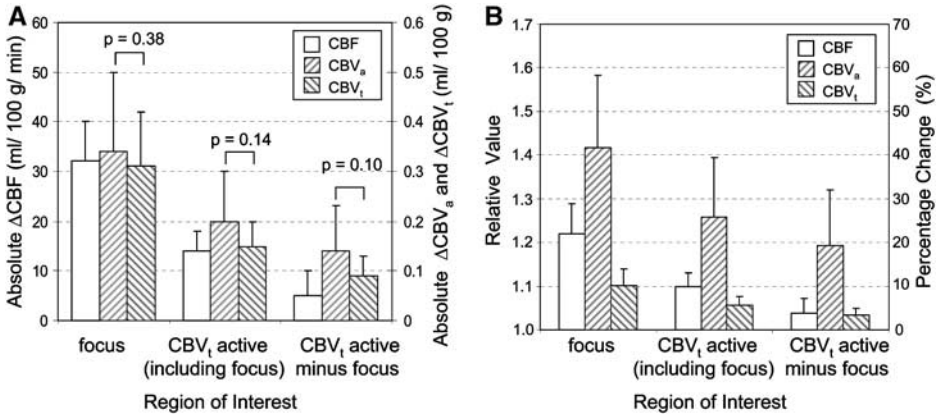

Figure 2 Regional quantification of absolute changes and relative hemodynamic values for ROIs of varying spatial extent. Analysis was performed for the contralateral ROIs indicated in Figure 1D to examine the ratios between hemodynamic measurements. (**A**) Although absolute changes are smaller in regions more remote from the activation focus because of a partial volume effect, there is no statistical difference between absolute change in CBV_a versus absolute change in CBV_t for any of the chosen ROIs. (**B**) The ratio of relative CBV_a versus relative CBV_t is also consistent for all ROIs ($P > 0.05$). This indicates that the blood volume change during neural activation is mainly due to arterial volume change rather than venous volume change and this result is independent of the ROI spatial extent.

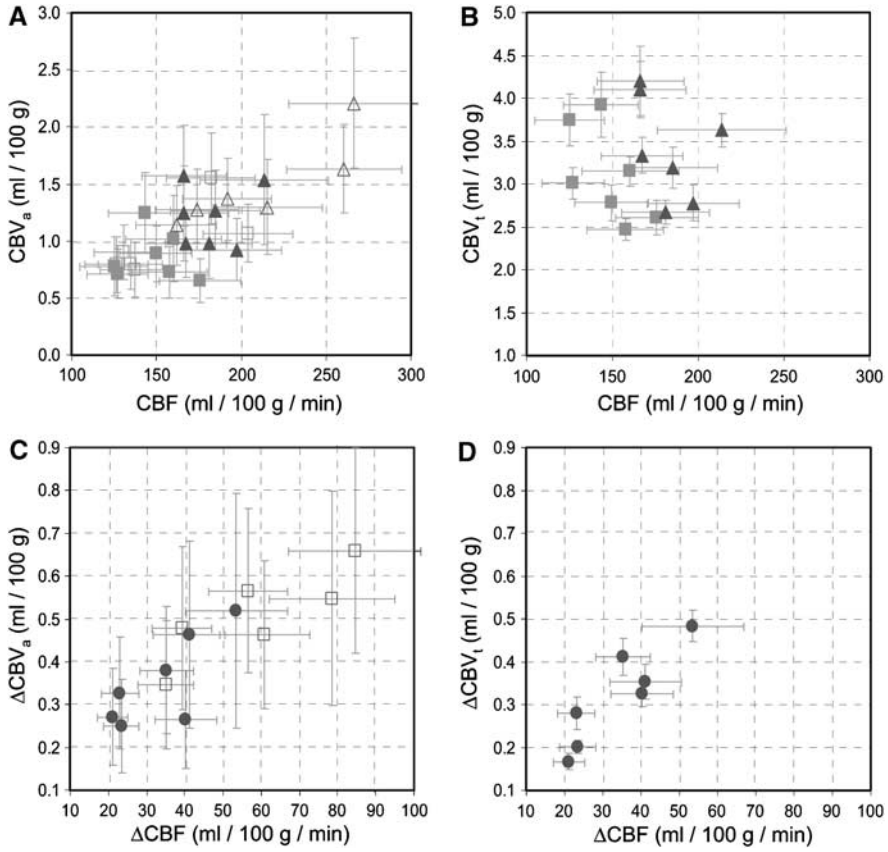

Figure 3 *Inter-animal* comparisons between values and changes to CBV_a and CBV_t versus *CBF* from within the 'focus ROI'. Open symbols represent data without subsequently measured CBV_t ($n = 6$) and filled symbols represent data with CBV_t measurements ($n = 7$). Data from baseline (squares) and stimulation (triangles) conditions for CBV_a versus *CBF* (**A**) and for CBV_t versus *CBF* (**B**) show scatter because of animal-to-animal variation, but all values are increased during stimulation and ΔCBF is highly correlated with both ΔCBV_a and ΔCBV_t, as can be more clearly seen when the stimulus-induced changes (circles) are plotted (**C**, **D**); a linear fit to this data yields ΔCBV_a (mL/100 g) = 0.008 (min) · ΔCBF (mL/100 g/min), $R = 0.87$, and ΔCBV_t (mL/100 g) = 0.009 (min) · ΔCBF (mL/100 g/min), $R = 0.89$. Error bars were determined by the error propagation analysis for each animal.

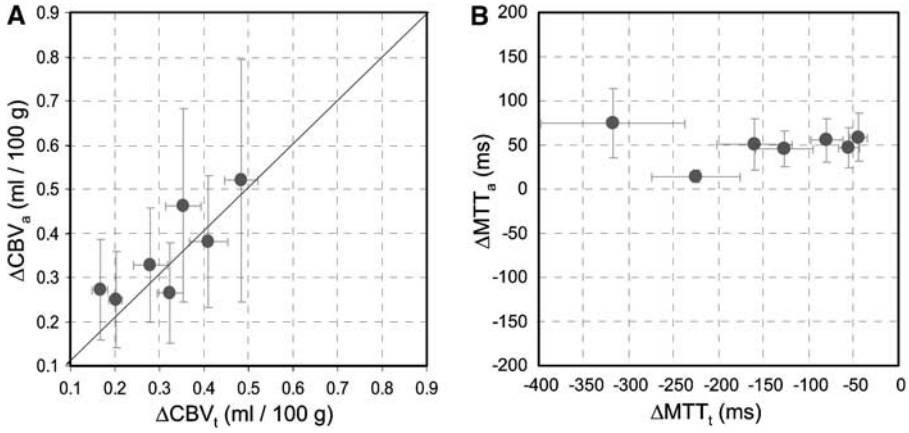

Figure 4 *Inter-animal* comparisons between stimulus-induced changes in CBV_a versus CBV_t (**A**) and MTT_a versus MTT_t (**B**) from the 'focus' ROI. (**A**) ΔCBV_t (mL/100 g) = 0.90 ΔCBV_a (mL/100 g), $R = 0.83$. Values for ΔCBV_a versus ΔCBV_t are not statistically different (paired *t*-test, $P > 0.05$). A line of identity is shown. (**B**) Negative values for ΔMTT_t (-144 ± 99 msecs) indicate a stimulus-induced increase in total blood velocity, while the small ΔMTT_a values ($+49 \pm 18$ msecs) suggest there is only very minor change to arterial blood velocity. Bars represent results of error propagation analysis for each animal.

and relationships between these stimulus-induced changes are highly correlated. *Inter-animal* comparisons for the 'focus' ROI are also plotted for arterial versus total CBV changes (Figure 4A), and for stimulus-induced changes in MTT_t (ΔMTT_t) and MTT_a (ΔMTT_a) (Figure 4B). These *inter-animal* comparisons further illustrate the dominance of the ΔCBV_a contribution to ΔCBV_t, and suggest a stimulus-induced increase in total blood velocity, but not arterial blood velocity.

Discussion

Technical Considerations in Arterial Cerebral Blood Volume and Total Cerebral Blood Volume Measurements

If there were significant CBV_v changes during stimulation, then ΔCBV_t would exceed ΔCBV_a. However, no significant differences between ΔCBV_a and ΔCBV_t were detected in our studies (Figure 2A), raising questions about possible errors in the measured values of CBV_a and/or CBV_t. We will first evaluate CBV_a quantification errors based on potential contributions from (i) venous blood signal; (ii) stimulation-induced changes in oxygenation and in exchange between blood and tissue water pools; and (iii) MT effects in arterial blood.

The contribution of venous volume to the CBV_a values will be negligible if labeled blood water in capillaries freely exchanges with tissue water during the spin tagging time; in this case, the exchange fraction (E, often referred to as the 'extraction fraction') will be equal to 1. If labeled blood water does not freely exchange with tissue water, some labeled water remains in the capillary, and venous blood then contributes to the CBV_a quantification. To evaluate this potential error, we expand our biophysical model from two compartments (artery and tissue) to four compartments (artery, capillary, tissue, and vein). Signal sources then consist of labeled spins in the arterial blood water pool, labeled spins in the tissue pool, and any labeled spins remaining in both the capillary and venous pools. Thus, the intensity difference between arterial labeled and unlabeled images (ΔS_{MT}) can be described as

$$\begin{aligned}\Delta S_{\mathrm{MT}} = & v_a 2\alpha_a M_0 \mathrm{e}^{-R_{2,\mathrm{artery}}\cdot TE} \\ & + v_c[C\cdot M_{\mathrm{MT}} + 2\alpha_c(1-E)M_0]\mathrm{e}^{-R_{2,\mathrm{capillary}}\cdot TE} \\ & + v_v[C\cdot M_{\mathrm{MT}} + 2\alpha_v(1-E)M_0]\,\mathrm{e}^{-R_{2,\mathrm{vein}}\cdot TE} \\ & + (1-v_a-v_c-v_v)C\cdot M_{\mathrm{MT}}\,\mathrm{e}^{-R_{2,\mathrm{tissue}}\cdot TE}\end{aligned} \quad (4)$$

where the spin fractions of arterial (v_a), capillary (v_c) and venous blood (v_v) are assumed to be 1%, 1%, and 3%, respectively; spin-labeling efficiencies in arterial (α_a), capillary (α_c), and venous (α_v) compartments are 0.36, 0.31, and 0.26, respectively (Kim and Kim, 2005); M_0 is the magnetization without MT and without spin labeling; M_{MT} is the magnetization with MT and without spin labeling; $R_{2,\mathrm{artery}}$ and $R_{2,\mathrm{tissue}}$ are the transverse relaxation rates (R_2 values) of arterial and tissue blood, which are both assumed to be 25 secs^{-1} (Lee *et al*, 1999); venous R_2 ($R_{2,\mathrm{vein}}$) is determined from 478–(458 · Y) secs^{-1} (Lee *et al*, 1999), where Y is the venous oxygenation level; capillary blood R_2 ($R_{2,\mathrm{capillary}}$) is assumed to be the averaged value of artery and vein; C is a constant related to blood flow, which is equivalent to

$$\left(2\alpha_c \frac{CBF}{\lambda}E\right)\Big/\left(\frac{1}{T_1}+\frac{CBF}{\lambda}E\right),$$

and is measured from the slope of normalized arterial spin-labeled signal change versus normalized unlabeled signals as a function of MT level and

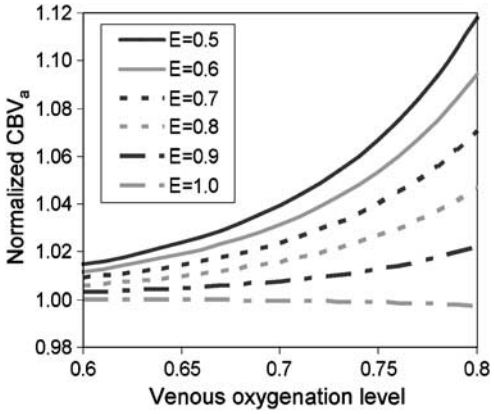

Figure 5 Simulation of CBV_a quantification errors with the two-compartment model, in the case that arterial spin-labeled water does not completely exchange with tissue. Two signal sources (artery and tissue) in the original biophysical model for measurement of CBV_a by MOTIVE are expanded to include four compartments, artery, capillary, tissue, and vein. See text for simulation parameters and assumptions. The overestimation of CBV_a is relatively small with the two-compartment model.

is assumed to be 0.033. Simulations performed with TE of 40 msecs for various venous oxygenation levels and exchange fractions that cover a range of reasonable expectations are graphed in Figure 5. Overestimation of CBV_a as calculated from the two-compartment model used in Results is relatively small.

Also, during neural stimulation, an elevation of *CBF* may cause a decrease in the water exchange fraction in capillaries and an increase in venous oxygenation level, resulting in an overestimation in ΔCBV_a. Venous oxygenation levels during stimulation can be determined from *CBF* values at baseline and stimulation conditions using Fick's principle assuming no oxygen consumption change induced by stimulation. Baseline oxygenation levels were 0.58 ± 0.01 for venous blood in human brain (An and Lin, 2000) and 0.64 ± 0.14 ($n = 6$) for blood from the femoral vein in our studies. Therefore, a reasonable upper estimate of venous oxygenation levels for baseline conditions is 0.60 to 0.70, and the corresponding levels during stimulation will be 0.67 to 0.75. The water exchange fraction relevant to our studies can be obtained by determination of $E = 1 - \exp(-PS/CBF)$, where *PS* is the capillary permeability-surface product. Assuming $PS =$ 138 mL/100 g/min (Eichling *et al*, 1974), E will be 0.6 for the baseline *CBF* of 150 mL/100 g/min, and ~ 0.5 for the stimulation *CBF* value of 182 mL/100 g/min. These simulations show that for baseline conditions ($E = 0.6$, $Y = 0.60$ to 0.70), CBV_a is overestimated by 1% to 3%, while for stimulation conditions ($E = 0.5$, $Y = 0.67$ to 0.75), CBV_a is overestimated by 3% to 7%. True CBV_a assuming these reasonable oxygenation levels would then be 0.81 to 0.82 mL/100 g at baseline and 1.09 to 1.14 mL/100 g during the stimulation condition. The largest possible error for any studies would occur if there was no overestimation for baseline ($E = 1$), and the measured CBV_a value during stimulation was overestimated by 12% (see Figure 5, $E = 0.5$, $Y = 0.8$). If we apply these larger errors to our own measurements, true CBV_a would increase from 0.83 at baseline to only 1.04 mL/100 g during stimulation. When we correct for these varying estimates of CBV_a quantification errors, we find that true ΔCBV_a would be somewhere in the range of 0.21 (assuming largest error) to 0.33 mL/100 g (assuming smallest error).

Related to this overestimation of CBV_a is the slight increase in our calculated value of MTT_a because of stimulation (Figure 4B), which suggests a blood velocity decrease in *parenchymal* arterial vessels. This is not expected. Blood velocity was previously observed to increase in *pial* arterial vessels (Ngai and Winn, 1996; Ngai and Winn, 2002). The discrepancy may be at least partly because of errors in our quantification. When $E < 1$, not only is CBV_a overestimated, but also *CBF* is underestimated. For example, if E is decreased by 10% because of activation, our ΔCBF value is underestimated by 10%. A reduced exchange fraction because of stimulation would therefore cause ΔMTT_a to be overestimated and could explain the slight increase we determined for MTT_a.

With the MOTIVE approach, it is assumed that the MT effect in arterial blood is not significant. When protons in tissue macromolecules are saturated by RF pulses, their magnetization is transferred to tissue water protons, selectively reducing the tissue signal. But we assume that the arterial pool is only minimally affected, because of its small macromolecular content, and because of the inflow of fresh spins from outside the B_1 field of MT-inducing pulses. Magnetization during an MT saturation time (t) reaches a steady state at the rate of $1/T_{1sat}$, where T_{1sat} is the apparent T_1 for equilibration of water and macromolecular pools; this magnetization can be expressed as $M_{MT}(t) = M_a \exp(-t/T_{1sat}) + M_s$, where M_a is the magnitude of magnetization decay and M_s is the magnetization residue at steady state, such that $M_{MT}(0) = M_a + M_s$; $M_{MT}(\infty) = M_s$ (Niemi *et al*, 1992). The MTR in stationary blood relative to gray matter is $\sim 40\%$ (Niemi *et al*, 1992; Pike *et al*, 1992), and therefore when MTR $(= 1 - M_{MT}(t)/M_{MT}(0) = 1 - S_{MT}(t)/S_{MT}(0))$ is 0.5 in gray matter (the highest MTR value in our studies), MTR of stationary blood is expected to be ~ 0.2. Using the same pulse power level, which gave an MTR value of 0.5 for gray matter, our own MR measurement on stationary blood yielded $M_{MT}(t) = 0.21 \cdot \exp(-t/1.87) + 0.79$ ($n = 1$, data not shown), where T_{1sat} is 1.87 secs. This fitting is well matched with estimates from literature (Niemi *et al*, 1992; Wolff and Balaban, 1989). In our specific application, the B_1 field from the head coil did not extend to the position of ASL in the animal's neck. Labeled arterial blood water will travel to the imaging plane in ~ 300 msecs (and so will experience the MT-inducing pulse for < 300 msecs), and then will spend ~ 300 msecs in the arterial vasculature of

the imaging pixel before exchange in the capillaries (Kim and Kim, 2006). Thus, the time that moving blood in arterial vessels experiences the MT-inducing B_1 field is within the range of 300 to 600 msecs, which gives M_{MT} ($t = 0.3$ to 0.6) = 0.97 to 0.94, with a resultant MTR range of 0.03 to 0.06. Therefore, in our measurements the signal reduction because of MT effects in arterial blood is negligible ($\sim$3% to 6% in arterial blood versus 50% in gray matter).

A potential error in CBV_t quantification is because of its determination by injection of a susceptibility contrast agent, which distributes only in plasma. Since we could not measure hematocrit levels from the cortical tissue of our MRI pixels, systemic *Hct* levels were instead measured to convert from plasma volume to whole blood volume (CBV_t) in our studies (see the factor $(1-Hct)$ in Equation (3)). However, capillary *Hct* level values have been reported to be 74% (Cremer and Seville, 1983) and 81% (Levin and Ausman, 1969) of systemic *Hct* levels. Therefore, the error in CBV_t quantification depends on the ratio of volumes between capillaries and large vessels, but the measurement of capillary volume is not trivial. If the capillary:large vessel volume ratio is 1:3, then CBV_t will be overestimated by 3% to 4%, whereas if the volume ratio is 1:1, then CBV_t will be overestimated by 5% to 7%. If the capillary volume is dominant, then CBV_t will be overestimated by 10% to 14%, which represents the upper limit of CBV_t error. If we assume that the *Hct* level does not change during stimulation, then ΔCBV_t will be similarly overestimated. After correction for this overestimation (i.e., 3% to 14%), ΔCBV_t is between 0.26 and 0.30 mL/100 g. An additional assumption is that the signal intensity of pixels is not influenced by static magnetic susceptibility effects from neighboring pixels. However, in our CBV_t maps, pixels in the region near large vessels will experience susceptibility effects from neighboring vessels, and thus CBV_t values in those pixels will be overestimated by an unknown amount. In our studies, the deoxyhemoglobin contribution to stimulus-induced CBV_t changes were removed; ΔCBV_t calculated without the correction of deoxyhemoglobin contribution would have been underestimated by $\sim$20%. Variation of stimulation-induced deoxyhemoglobin changes will also affect ΔCBV_t. In our studies, the intra-animal, inter-run s.d. of BOLD signals was 42% of its mean, which will give $\sim$8% error (0.42×0.2) in ΔCBV_t values.

Relationships between Arterial Cerebral Blood Volume and Total Cerebral Blood Volume

The ratio of baseline CBV_a to CBV_t for normal physiological conditions has previously been a parameter of interest. Our CBV_a/CBV_t value was 0.27 ± 0.05, which is consistent with 0.29 ± 0.07 in halothane-anesthetized rats (Duong and Kim, 2000), 0.25 in α-chloralose-anesthetized rats (Lee *et al*, 2001), and 0.23 ± 0.04 in humans (An and Lin, 2002). However, these CBV_a/CBV_t values measured by NMR spectroscopy or MRI are lower than the values determined by PET in humans of 0.37 ± 0.11 (Ito *et al*, 2001*a*) and 0.46 ± 0.12 (Ito *et al*, 2005). Interestingly, although there is a large difference in baseline *CBF* between isoflurane and α-chloralose anesthetics ($\sim$150 versus $\sim$60 mL/100 g/min), values of CBV_a/CBV_t are similar. This suggests that isoflurane effects on arterial and venous vessels may be similar.

During neural activation, the CBV_a change is dominant, while the CBV_v change is negligible. Our quantitative relationship between CBV_a and CBV_t data in this rat study during 15 secs of somatosensory stimulation agrees reasonably well with human PET studies during global stimulation (Ito *et al*, 2005). If overestimation errors in ΔCBV_a outweigh overestimation errors in ΔCBV_t, then there could actually be a CBV_v increase. In our laboratory's previous *CBF* and CBV_v measurements with ^{19}F NMR spectroscopy, CBV_v was slightly increased during elevated *CBF* in α-chloralose anesthetized rats during steady-state, high $PaCO_2$ conditions (Lee *et al*, 2001). The discrepancy in measured CBV_v changes in the two studies might be because of different anesthetics (isoflurane versus α-chloralose), different spatial distributions of activation (somatosensory cortex versus whole brain), different physiological origins of response (CO_2 or H+ versus neural activity), different stimulus durations (short forepaw stimulation versus long CO_2 inhalation), different baseline *CBF* values, and/or measurement errors that differ with technique.

Arterial and venous CBV changes can also be inferred from vessel diameter measurements. Most measurements have been performed on pial vessels because of limitations in microscopic vessel visualization. Direct *pial* vessel diameter measurements during hypercapnia showed increases of $\sim$58% in 10 to 20 μm diameter arterial vessels versus $\sim$10% increases in 10 to 20 μm diameter venous vessels (Lee *et al*, 2001). Using the 2D optical imaging spectroscopy technique, Berwick *et al* (2005) found that blood volume changes during rodent whisker-stimulation were larger in arterial pial vessels than in venous pial vessels by a ratio of 2.9. Recently, Takano *et al* (2006) measured changes of *parenchymal* vessels in mouse somatosensory cortex using two-photon microscopy; arterial vessel diameter increased $\sim$18% during stimulation, while venous vessel diameter increased $\sim$2%. These microscopic measurements of vessels indicate that arterial blood volume change is dominant during neural stimulation, which is consistent with our observations.

Our finding may not be applicable to all stimulation studies. The magnitude of time-dependent CBV_v change may depend on stimulation type and duration. Stefanovic and Pike reported a 16% CBV_v increase in humans during 4-min-long radial yellow/blue checkerboard stimulation at 4 Hz reversing frequency (Stefanovic and Pike, 2005). In their measurement, many assumptions are required to

separate the venous blood volume change from transverse relaxation changes in tissue and blood. Since venous blood vessels passively respond to upstream blood pressure, the dynamics of CBV_v are likely to be slower than those of CBV_a (Mandeville *et al*, 1999). Thus, stronger and longer stimulation is likely to result in a higher CBV_v response at a later time.

Implication for Blood Oxygenation Level Dependent Quantification

The relationship between R_2^* and deoxyhemoglobin (the source of BOLD signal) has been extensively investigated. In short, the BOLD effect depends on venous oxygenation level (Y) and CBV_v (Ogawa *et al*, 1993). Assuming that the intravascular blood signal contribution is minimal and arterial blood is fully oxygenated, R_2^* can be expressed as $R_2^* = a \cdot \mathrm{CBV}_v \cdot (1-Y)^\beta$, where a and β are constants (Ogawa *et al*, 1993). The multiplier a is related to vessel orientation, magnetic field strength, susceptibility difference between fully oxygenated and deoxygenated blood, hematocrit level, and pulse sequence (SE versus GE). The exponent β depends on vessel size and on the frequency shift due to deoxyhemoglobin, and is related to the relative contribution of the diffusion effect, with $1 \leqslant \beta \leqslant 2$; $\beta = 1$ for the static-dephasing domain, while $\beta = 2$ for the free diffusion domain.

Increased neural activity induces a change in venous blood oxygenation level (ΔY) and a change in venous blood volume (ΔCBV_v); $\Delta R^*_{2,\mathrm{stim}} = a \cdot (CBV_v + \Delta CBV_v) \cdot (1-Y-\Delta Y)^\beta - aCBV_v \cdot (1-Y)^\beta$. Using a first-order Taylor expansion,

$$\Delta R^*_{2,\mathrm{stim}} = -a\beta(1-Y)^\beta CBV_v \times \left\{ \frac{\Delta Y}{1-Y} - \frac{1}{\beta}\frac{\Delta CBV_v}{CBV_v} \right\} \quad (5)$$

(see Kim *et al*, 1999 for a detailed derivation). $\Delta CBV_v/CBV_v$ has previously been estimated either directly from $\Delta CBV_t/CBV_t$ measurements (Mandeville *et al*, 1998) or indirectly from CBF changes using $rCBV_t = rCBV_v = rCBF^k$ (Davis *et al*, 1998; Kim and Ugurbil, 1997). Since our results show relatively small or negligible venous blood volume changes during stimulation ($\Delta CBV_v \cong 0$), BOLD fMRI signals under our conditions arise mostly from changes in venous oxygenation (ΔY). If the relationship $\Delta CBV_v/CBV_v = \Delta CBV_t/CBV_t$ is used in Equation (5), ΔY will be overestimated as determined from the measured BOLD response, and this overestimation in ΔY consequently translates into an underestimation of $\Delta CMRO_2/\mathrm{CMRO}_2$. Therefore, accurate determination of venous CBV change is important in quantification of physiological parameters from BOLD fMRI signal changes.

Conclusions

We have successfully quantified CBF, CBV_a and CBF_t during control and stimulation periods. Under our conditions of 15-s somatosensory stimulation in isoflurane-anesthetized rats, we determined that coincident with the neural-induced elevation of CBF, blood volume changes occur mainly in arteries rather than in veins. Since arterial and venous CBV changes can be dependent on stimulation duration and type, extensive studies are needed before our observation can be generalized.

References

An H, Lin W (2000) Quantitative measurements of cerebral blood oxygen saturation using magnetic resonance imaging. *J Cereb Blood Flow Metab* 20:1225–36

An H, Lin W (2002) Cerebral venous and arterial blood volumes can be estimated separately in humans using magnetic resonance imaging. *Magn Reson Med* 48:583–8

Bandettini PA, Jesmanowicz A, Wong EC, Hyde JS (1993) Processing strategies for time-course data sets in functional MRI of the human brain. *Magn Reson Med* 30:161–73

Barbier EL, Lamalle L, Decorps M (2001) Methodology of brain perfusion imaging. *J Magn Reson Imaging* 13:496–520

Berwick J, Johnston D, Jones M, Martindale J, Redgrave P, McLoughlin N, Schiessl I, Mayhew JE (2005) Neurovascular coupling investigated with two-dimensional optical imaging spectroscopy in rat whisker barrel cortex. *Eur J Neurosci* 22:1655–66

Buxton RB, Wong EC, Frank LR (1998) Dynamics of blood flow and oxygenation changes during brain activation: the balloon model. *Magn Reson Med* 39:855–64

Chu SC, Xu Y, Balschi JA, Springer CS, Jr (1990) Bulk magnetic susceptibility shifts in NMR studies of compartmentalized samples: use of paramagnetic reagents. *Magn Reson Med* 13:239–62

Cremer JE, Seville MP (1983) Regional brain blood flow, blood volume, and haematocrit values in the adult rat. *J Cereb Blood Flow Metab* 3:254–6

Davis TL, Kwong KK, Weisskoff RM, Rosen BR (1998) Calibrated functional MRI: mapping the dynamics of oxidative metabolism. *Proc Natl Acad Sci USA* 95:1834–9

Dodd SJ, Williams M, Suhan JP, Williams DS, Koretsky AP, Ho C (1999) Detection of single mammalian cells by high-resolution magnetic resonance imaging. *Biophys J* 76:103–9

Duong TQ, Kim SG (2000) *In vivo* MR measurements of regional arterial and venous blood volume fractions in intact rat brain. *Magn Reson Med* 43:393–402

Eichling JO, Raichle ME, Grubb RL, Jr, Ter-Pogossian MM (1974) Evidence of the limitations of water asa freely diffusible tracer in brain of the rhesus monkey. *Circ Res* 35:358–64

Grubb RL, Jr, Raichle ME, Eichling JO, Ter-Pogossian MM (1974) The effects of changes in PaCO2 on cerebral blood volume, blood flow, and vascular mean transit time. *Stroke* 5:630–9

Herscovitch P, Raichle ME (1985) What is the correct value for the brain–blood partition coefficient for water? *J Cereb Blood Flow Metab* 5:65–9

Iadecola C, Yang G, Ebner TJ, Chen G (1997) Local and propagated vascular responses evoked by focal synaptic activity in cerebellar cortex. *J Neurophysiol* 78: 651–9

Ito H, Ibaraki M, Kanno I, Fukuda H, Miura S (2005) Changes in the arterial fraction of human cerebral blood volume during hypercapnia and hypocapnia measured by positron emission tomography. *J Cereb Blood Flow Metab* 25:852–7

Ito H, Kanno I, Iida H, Hatazawa J, Shimosegawa E, Tamura H, Okudera T (2001*a*) Arterial fraction of cerebral blood volume in humans measured by positron emission tomography. *Ann Nucl Med* 15:111–6

Ito H, Takahashi K, Hatazawa J, Kim SG, Kanno I (2001*b*) Changes in human regional cerebral blood flow and cerebral blood volume during visual stimulation measured by positron emission tomography. *J Cereb Blood Flow Metab* 21:608–12

Jones M, Berwick J, Mayhew J (2002) Changes in blood flow, oxygenation, and volume following extended stimulation of rodent barrel cortex. *Neuroimage* 15:474–87

Kennan RP, Scanley BE, Innis RB, Gore JC (1998) Physiological basis for BOLD MR signal changes due to neuronal stimulation: separation of blood volume and magnetic susceptibility effects. *Magn Reson Med* 40:840–6

Kim SG, Rostrup E, Larsson HB, Ogawa S, Paulson OB (1999) Determination of relative CMRO2 from CBF and BOLD changes: significant increase of oxygen consumption rate during visual stimulation. *Magn Reson Med* 41:1152–61

Kim SG, Ugurbil K (1997) Comparison of blood oxygenation and cerebral blood flow effects in fMRI: estimation of relative oxygen consumption change. *Magn Reson Med* 38:59–65

Kim T, Kim SG (2002) Dynamics of arterial labeled spins investigated by using 2-coil DASL. *Proceedings of the 10th Annual Meeting* ISMRM, Hawaii, USA, p. 1061

Kim T, Kim SG (2005) Quantification of cerebral arterial blood volume and cerebral blood flow using MRI with modulation of tissue and vessel (MOTIVE) signals. *Magn Reson Med* 54:333–42

Kim T, Kim SG (2006) Quantification of cerebral arterial blood volume using arterial spin labeling with intravoxel in coherent motion-sensitive gradients. *Magn Reson Med* 55:1047–57

Lee SP, Duong TQ, Yang G, Iadecola C, Kim SG (2001) Relative changes of cerebral arterial and venous blood volumes during increased cerebral blood flow: implications for BOLD fMRI. *Magn Reson Med* 45:791–800

Lee SP, Silva AC, Ugurbil K, Kim SG (1999) Diffusion-weighted spin-echo fMRI at 9.4 T: microvascular/tissue contribution to BOLD signal changes. *Magn Reson Med* 42:919–28

Levin VA, Ausman JI (1969) Relationship of peripheral venous hematocrit to brain hematocrit. *J Appl Physiol* 26:433–7

Lukasik VM, Gillies RJ (2003) Animal anaesthesia for *in vivo* magnetic resonance. *NMR Biomed* 16:459–67

Maekawa T, Tommasino C, Shapiro HM, Keifer-Goodman J, Kohlenberger RW (1986) Local cerebral blood flow and glucose utilization during isoflurane anesthesia in the rat. *Anesthesiology* 65:144–51

Mandeville JB, Marota JJ, Kosofsky BE, Keltner JR, Weissleder R, Rosen BR, Weisskoff RM (1998) Dynamic functional imaging of relative cerebral blood volume during rat forepaw stimulation. *Magn Reson Med* 39:615–24

Mandeville JB, Marota JJA, Ayata C, Zaharchuk G, Moskowitz MA, Rosen B, Weisskoff R (1999) Evidence of a cerebrovascular postarteriole windkessel with delayed compliance. *J Cereb Blood Flow Metab* 19:679–89

Mandeville JB, Moore J, Chesler DA, Garrido L, Weissleder R, Weisskoff RM (1997) Dynamic liver imaging with iron oxide agents: effects of size and biodistribution on contrast. *Magn Reson Med* 37:885–90

Masamoto K, Kim T, Fukuda H, Wang P, Kim SG (In press) Relationship between neural, vascular, and BOLD signals in isoflurane-anesthetized rat somatosensory cortex. *Cerebral Cortex*, 2006 May 26 [Epub ahead of print] doi:10.1093/cercor/bh1005

Nakai K, Imai H, Kamei I, Itakura T, Komari N, Kimura H, Nagai T, Maeda T (1981) Microangioarchitecture of rat parietal cortex with special reference to vascular 'sphincters'. Scanning electron microscopic and dark field microscopic study. *Stroke* 12:653–9

Ngai AC, Winn HR (1996) Estimation of shear and flow rates in pial arterioles during somatosensory stimulation. *Am J Physiol* 270:H1712–7

Ngai AC, Winn HR (2002) Pial arteriole dilation during somatosensory stimulation is not mediated by an increase in CSF metabolites. *Am J Physiol Heart Circ Physiol* 282:H902–7

Niemi PT, Komu ME, Koskinen SK (1992) Tissue specificity of low-field-strength magnetization transfer contrast imaging. *J Magn Reson Imaging* 2:197–201

Ogawa S, Menon RS, Tank DW, Kim S-G, Merkle H, Ellermann JM, Ugurbil K (1993) Functional brain mapping by blood oxygenation level-dependent contrast magnetic resonance imaging. *Biophys J* 64:800–12

Paxinos G, Watson C (1986) *The rat brain in sterotaxic coordinates*. San Diego: Academic Press

Pike GB, Hu BS, Glover GH, Enzmann DR (1992) Magnetization transfer time-of-flight magnetic resonance angiography. *Magn Reson Med* 25:372–9

Sanders JA, Orrison WW (1995) Functional magnetic resonance imaging. In: *Functional Brain Imaging* (Orrison WW, Lewine JD, Sanders JA, Hartshorne MF, eds), St Louis: Mosby

Silva AC, Lee SP, Iadecola C, Kim SG (2000) Early temporal characteristics of cerebral blood flow and deoxyhemoglobin changes during somatosensory stimulation. *J Cereb Blood Flow Metab* 20:201–6

Spees WM, Yablonskiy DA, Oswood MC, Ackerman JJ (2001) Water proton MR properties of human blood at 15 Tesla: magnetic susceptibility, T_1,T_2,T_2* and non-Lorentzian signal behavior. *Magn Reson Med* 45:533–42

Stefanovic B, Pike GB (2005) Venous refocusing for volume estimation: VERVE functional magnetic resonance imaging. *Magn Reson Med* 53:339–47

Takano T, Tian GF, Peng W, Lou N, Libionka W, Han X, Nedergaard M (2006) Astrocyte-mediated control of cerebral blood flow. *Nat Neurosci* 9:260–7

Tropres I, Grimault S, Vaeth A, Grillon E, Julien C, Payen JF, Lamalle L, Decorps M (2001) Vessel size imaging. *Magn Reson Med* 45:397–408

Weisskoff RM, Kiihne S (1992) MRI susceptometry: image-based measurement of absolute susceptibility of MR contrast agents and human blood. *Magn Reson Med* 24:375–83

Wolff SD, Balaban RS (1989) Magnetization transfer contrast (MTC) and tissue water proton relaxation *in vivo*. *Magn Reson Med* 10:135–44

Yablonskiy DA, Haacke EM (1994) Theory of NMR signal behavior in magnetically inhomogeneous tissues: the static dephasing regime. *Magn Reson Med* 32:749–63

Zhao F, Wang P, Hendrich KS, Ugurbil K, Kim SG (2006) Cortical layer-dependent BOLD and CBV responses measured by spin-echo and gradient-echo fMRI: insights into hemodynamic regulation. *NeuroImage* 30:1149–60